JOURNAL OF MATERIALS SCIENCE 20 (1985) 2233–2244

Calculation of the solid–liquid interfacial tension in metallic ternary systems

D. CHATAIN, D. PIQUE, L. COUDURIER, N. EUSTATHOPOULOS
Laboratoire de Thermodynamique et Physico-Chime Métallurgiques, E.N.S.E.E.G., Domaine Universitaire, B.P. 75, 38402 Saint Martin d'Hères Cédex, France

We present a two-layer interface model for calculating the interfacial tension and adsorption of a solid A–liquid B–solute C system from the phase diagram and the thermodynamic mixing data of liquid alloys of the three AB, BC and AC systems. This model correctly predicts the isotherms "interfacial tension versus composition" over the whole ternary range where a solid and a liquid coexist. From this model, we establish a tensioactivity criterium for the infinitely dilute solute C at the solid–liquid interface. This is in good agreement with the measurements of interfacial activity in systems studied with iron, aluminium or zinc-based solid phase.

1. Introduction

The knowledge of the energetic properties of solid–liquid interfaces in multicomponent systems, is of a great interest in materials science because such interfaces play an important part in nucleation and crystal growth of melts, wetting phenomena and brazing, liquid-phase sintering, and embrittlement of solids by liquid metals.

This explains the numerous models for calculation of solid–liquid interfacial tension that have been presented by many authors over the last ten years [1–5]. However, in view of the difficulties in correctly describing the atomic structure of metal solid–liquid interfaces, these models are restricted to simple binary systems. For many applications, however, multicomponent systems must generally be considered, and it is of particular interest to know the influence of a third element on the interfacial tension of a solid A–liquid B-based system.

As the complexity of description of metallic systems increases very rapidly with the number of components, we present for ternary systems, a model based on several simplifying but physically justified assumptions, in order to extract the principal factors determining the tensioactivity at solid–liquid interfaces.

2. The interfacial model

For calculating the interfacial tension of an A–B–C system (where the major component of the solid is the metal A) we use atomistic models based on the following assumptions:

1. the interactions are restricted to the nearest neighbouring atoms; and

2. the atoms of the liquid phase are on the sites of a crystalline-like lattice which is isomophoric and coherent with that of the solid phase.

The interface is represented by two monatomic layers, one liquid, the other solid. This choice is supported by the works on binary systems of Camel *et al.* [6] and Passerone and Eustathopoulos [7] who showed that at low temperatures ($T/T_m^A \ll 1$) the interface of these systems is atomically smooth and becomes rough only near the melting temperature, T_m^A, of the major element of the solid phase. Moreover, Coudurier *et al.* [8], using a multilayer model, have shown that two layers (which is the minimum thickness of an atomically smooth solid–liquid interface) are generally sufficient to describe the composition profile at the interface of binary systems, except in the temperature range where instability of the liquid exists (miscibility gap).

The A–B–C solid–interface–liquid system is

0022–2461/85 $03.00 + .12 © *1985 Chapman and Hall Ltd.*

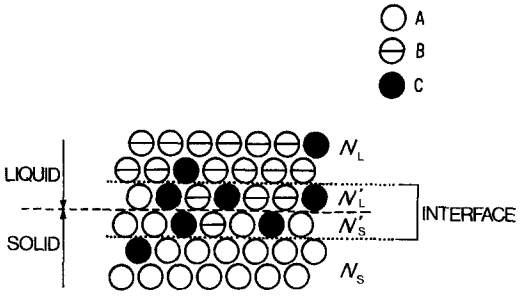

Figure 1 Two layer model of solid–liquid interfaces of a ternary system.

represented in Fig. 1: the number of atoms in each bulk phase j and in each interfacial layer j are, respectively, N_i^j and N'^j_i with $N'/N \ll 1$.

3. Interfacial tension

3.1. Expression

The free energy of such a system at equilibrium is given by [9]:

$$F = -PV + \sigma\Omega + \sum_i \sum_j [(N^j x_i^j + N'^j y_i^j)\mu_i^j] \tag{1}$$

where P is the pressure of the system, V, the volume, σ, the interfacial tension, Ω the interfacial area, x_i^j, y_i^j, the molar fractions of i in the bulk phase j and in the interfacial layer j, respectively, μ_i^j, the chemical potential of i in the phase j.

As the two phases are condensed, the term PV is negligible compared with the energy of the system [9], and the expression of the interfacial tension is then:

$$\sigma = \frac{1}{\Omega}\left[F - \sum_i \sum_j ((N^j x_i^j + N'^j y_i^j)\mu_i^j)\right] \tag{2}$$

For calculating F and μ_i^j, which is a partial derivative of F:

$$\mu_i^j = \left(\frac{\partial F}{\partial N_i^j}\right)_{T,V,N_{i'}^j \neq i} \tag{3}$$

Bragg and Williams statistics are used: they assume a perfectly disordered distribution of the atoms on the different sites of each phase. The free energy, F, is calculated from the partition function, ϕ:

$$F = -kT \ln \phi \tag{4}$$

with

$$\phi = \prod_j \frac{N^j!}{\prod_i N_i^j!} \cdot \frac{N'^j!}{\prod N'^j_i!} \exp\left(-\frac{\bar{E}}{kT}\right) \tag{5}$$

where k is the Boltzman constant and $\bar{E}$ the configurational energy of a perfectly disordered system. $\bar{E}$ can be decomposed into four terms:

$$\bar{E} = E^S + E^L + E'^S + E'^L \tag{6}$$

E^j is the configurational energy of the phase j containing N^j atoms, and E'^j the same energy of the interfacial layer j containing N'^j atoms. Each term is calculated by additioning the energy of all the pairs of atoms:

$$E^j = \frac{z}{2}(N^j - mN'^j)\,[\epsilon_{AA}^j x_A^{j\,2} + \epsilon_{BB}^j x_B^{j\,2} + \epsilon_{CC}^j x_C^{j\,2} + 2\epsilon_{AB}^j x_A^j x_B^j + 2\epsilon_{BC}^j x_B^j x_C^j + 2\epsilon_{AC}^j x_A^j x_C^j] \tag{7a}$$

$$E'^j = zN'^j \left\{ \frac{l}{2}(\epsilon_{AA}^j y_A^{j\,2} + \epsilon_{BB}^j y_B^{j\,2} + \epsilon_{CC}^j y_C^{j\,2} + 2\epsilon_{AB}^j y_A^j y_B^j + 2\epsilon_{BC}^j y_B^j y_C^j + 2\epsilon_{AC}^j y_A^j y_C^j) + m\,[\epsilon_{AA}^j y_A^j x_A^j + \epsilon_{BB}^j y_B^j x_B^j + \epsilon_{CC}^j y_C^j x_C^j + \epsilon_{AB}^j (y_A^j x_B^j + y_B^j x_A^j) + \epsilon_{BC}^j (y_B^j x_C^j + y_C^j x_B^j) + \epsilon_{AC}^j (y_A^j x_C^j + y_C^j x_A^j)] + \frac{m}{2}(\epsilon_{AA}^{SL} y_A^S y_A^L + \epsilon_{BB}^{SL} y_B^S y_B^L + \epsilon_{CC}^{SL} y_C^S y_C^L + \epsilon_{AB}^{SL} y_A^S y_B^L + \epsilon_{BC}^{SL} y_B^S y_C^L + \epsilon_{CA}^{SL} y_C^S y_A^L + \epsilon_{BA}^{SL} y_B^S y_A^L + \epsilon_{CB}^{SL} y_C^S y_B^L + \epsilon_{AC}^{SL} y_A^S y_C^L) \right\} \tag{7b}$$

where z is the coordination number, l, the fraction of the nearest neighbours located in the same layer parallel to the interface, and m in an adjacent one ($l + 2m = 1$), $\epsilon_{ii'}^j$, the energy of heteroatomic pair in the j-phase, and $\epsilon_{ii'}^{SL}$, the energy of the pair composed by an i solid atom and an i' liquid one ($\epsilon_{i'i}^{SL} \neq \epsilon_{ii'}^{SL}$).

By introducing the exchange energies $W_{ii'}^{jj'}$:

$$W_{ii'}^{jj'} = z\left(\epsilon_{ii'}^{jj'} - \frac{\epsilon_{ii}^j + \epsilon_{i'i'}^{j'}}{2}\right) \tag{8}$$

and putting $N'^S = N'^L = N'$ and $N^S = N^L = N$, the configurational energy is given by:

$$\bar{E} = \frac{z}{2}\sum_j [(N_A^j + N_A'^j)\,\epsilon_{AA}^j + (N_B^j + N_B'^j)\,\epsilon_{BB}^j + (N_C^j + N_C'^j)\,\epsilon_{CC}^j] + \sum_j N[x_A^j x_B^j W_{AB}^{jj} + x_B^j x_C^j W_{BC}^{jj} + x_A^j x_C^j W_{AC}^{jj}] + \frac{l}{2}\sum_j N'[y_A^j y_B^j W_{AB}^{jj} + y_B^j y_C^j W_{BC}^{jj} + y_A^j y_C^j W_{AC}^{jj}]$$

$$+ m\sum_j N'[(y_A^j x_B^j + y_B^j x_A^j - x_A^j x_B^j)\, W_{AB}^{jj} + (y_B^j x_C^j + y_C^j x_B^j - x_B^j x_C^j)\, W_{BC}^{jj} + (y_A^j x_C^j + y_C^j x_A^j - x_A^j x_C^j)\, W_{AC}^{jj}]$$
$$mN'(y_A^S y_A^L\, W_{AA}^{SL} + y_B^S y_B^L W_{BB}^{SL} + y_C^S y_C^L W_{CC}^{SL}) + mN'(y_A^S y_B^L W_{AB}^{SL} + y_B^S y_C^L W_{BC}^{SL} + y_C^S y_A^L W_{CA}^{SL} + y_B^S y_A^L W_{BA}^{SL} + y_C^S y_B^L W_{CB}^{SL} + y_A^S y_C^L W_{AC}^{SL}) \quad (9)$$

The different terms of this equation represent:

1. first term, the energy of a system where all the atoms are supposedly surrounded by atoms of the same chemical and physical state;
2. second term, the exchange energy associated with the formation of the solid and liquid bulk solutions;
3. third term, the exchange energy of the heteroatomic pairs *in* the interfacial layers;
4. fourth term, the exchange energy of the heteroatomic pairs made of one atom of the j interfacial layer and one atom located in the adjacent layer belonging to the j bulk phase;
5. fifth term, the exchange energy of the pairs made of chemically identical but physically different atoms; and
6. the last term, the exchange energy of pairs of both chemically and physically different atoms.

From this expression of $\bar{E}$, F can be calculated (Equations 4, 5) as the chemical potentials of each element i in the bulk phase j neglecting the terms in N'/N of Equation 9.

For example, for A we find:

$$\mu_A^j = \frac{z}{2}\epsilon_{AA}^j + kT\ln x_A^j + W_{AB}^{jj} x_B^{j\,2} + W_{AC}^{jj} x_C^{j\,2} + (W_{AB}^{jj} + W_{AC}^{jj} - W_{BC}^{jj})\, x_B^j x_C^j . \quad (10)$$

The expression of the interfacial tension is then:

$$\sigma\omega = kT\sum_j \left(y_A^j \ln\frac{y_A^j}{x_A^j} + y_B^j \ln\frac{y_B^j}{x_B^j} + y_C^j \ln\frac{y_C^j}{x_C^j}\right) + l\sum_j (y_A^j y_B^j W_{AB}^{jj} + y_B^j y_C^j W_{BC}^{jj} + y_A^j y_C^j W_{AC}^{jj}) + (m-1)\sum_j [(y_A^j x_B^j + y_B^j x_A^j - x_A^j x_B^j)\, W_{AB}^{jj} + (y_B^j x_C^j + y_C^j x_B^j - x_B^j x_C^j)\, W_{BC}^{jj} + (y_A^j x_C^j + x_A^j y_C^j - x_A^j x_C^j)\, W_{AC}^{jj}] + m(y_A^S y_A^L W_{AA}^{SL} + y_B^S y_B^L W_{BB}^{SL} + y_C^S y_C^L W_{CC}^{SL}) + m(y_A^S y_B^L W_{AB}^{SL} + y_B^S y_C^L W_{BC}^{SL} + y_C^S y_A^L W_{CA}^{SL} + y_B^S y_A^L W_{BA}^{SL} + y_C^S y_B^L W_{CB}^{SL} + y_A^S y_C^L W_{AC}^{SL}) \quad (11)$$

where ω is the atomic interfacial area ($\omega = \Omega/N'$).

All the energetic parameters $W_{ii'}^{jj'}$, which appear in Equations 10 and 11 are linked to physical quantities, the values of which can be found in the literature.

By putting $x_{i\neq i'} = y_{i\neq i'}$ in Equation 11, a relationship can be found between W_{ii}^{SL} and σ_i°:

$$m\mathcal{N}W_{ii}^{SL} = \sigma_i^\circ \Omega_M \quad (12)$$

where Ω_M is the molar interfacial area and $\mathcal{N}$ the Avogadro number.

The parameter $W_{ii'}^{jj}$ is replaced by its molar quantity $\lambda_{ii'}^j$ which is the molar exchange energy of the ii' corresponding regular binary solution:

$$\mathcal{N}W_{ii'}^{jj} = \lambda_{ii'}^j \quad (13)$$

The heteroatomic interactions across the interface $W_{ii'}^{jj'}$ are linked to the two others according to Coudurier *et al.* [10]:

$$\mathcal{N}W_{ii'}^{SL} = \mathcal{N}(W_{ii}^{SL} + W_{ii'}^{LL}) = \frac{\sigma_i^\circ \Omega_M}{m} + \lambda_{ii'}^L \quad (14)$$

Taking into account all these equations (Equations 12, 13 and 14), the expression of the interfacial tension becomes:

$$\sigma\Omega_M = y_A^S\sigma_A^\circ\Omega_M + y_B^S\sigma_B^\circ\Omega_M + y_C^S\sigma_C^\circ\Omega_M + RT\sum_j [y_A^j \ln(y_A^j/x_A^j) + y_B^j \ln(y_B^j/x_B^j) + y_C^j \ln(y_C^j/x_C^j)] + l\sum_j (\lambda_{AB}^j y_A^j y_B^j + \lambda_{BC}^j y_B^j y_C^j + \lambda_{CA}^j y_A^j y_C^j) + m\sum_{j\neq j'} (\lambda_{AB}^L y_A^j y_B^{j'} + \lambda_{BC}^L y_B^j y_C^{j'} + \lambda_{CA}^L y_A^j y_C^{j'}) - (l+m)\sum_j [\lambda_{AB}^j (y_A^j x_B^j + y_B^j x_A^j - x_A^j x_B^j) + \lambda_{BC}^j (y_B^j x_C^j + y_C^j x_B^j - x_B^j x_C^j) + \lambda_{CA}^j (y_C^j x_A^j + y_A^j x_C^j - x_C^j x_A^j)] \quad (15)$$

3.2. Estimation of the parameters

The interfacial molar area, Ω_M, is computed from the solid molar volume V_m:

$$\Omega_M = f\mathcal{N}\left(\frac{V_m}{\mathcal{N}}\right)^{2/3} \quad (16)$$

where f is a structural factor equal to 1.091 for the |111| plane of an fcc structure and the |0001| plane of an hc one, and equal to 1.12 for a |110| plane of a cc structure, these planes being the most densely packed planes of the corresponding structures. For all these orientations we have:

$$l = 2m = 1/2$$

The values of σ_i° are estimated by using the empirical equation deduced from existing data on the solid–liquid interfacial tension of pure metals [11]:

$$\sigma_i^\circ = 0.065 L_f^i (V_m^i)^{-2/3} \quad (\mathrm{mJ\,m^{-2}}) \quad (17)$$

where L_f is the heat of fusion in $\mathrm{J\,mol^{-1}}$ and V_m^i in $\mathrm{cm^3\,mol^{-1}}$.

The excess entropy of binary metallic solutions being generally not negligible, the $\lambda_{ii'}^L$ parameters are chosen equal to the mean value of the excess free energies at infinite dilution $\overline{\Delta G}_i^{xs\infty}$ and $\overline{\Delta G}_{i'}^{xs\infty}$ (subregular solutions). These quantities generally proceed from the Hultgren *et al.* complication [12]. For binary solid solutions, as thermodynamic quantities are very scarce, the parameters $\lambda_{ii'}^S$ are estimated from $\lambda_{ii'}^L$, and the ii' binary phase diagram by using the equation of equality of the chemical potentials of the minor element i' of the solid phase for the two phases in equilibrium:

$$\lambda_{ii'}^S = \left[RT \ln (x_{i'}^L/x_{i'}^S) + \lambda_{ii'}^L (x_i^L)^2 + L_f^{i'} \left(1 - \frac{T}{T_m^{i'}}\right)\right] \Big/ (x_i^S)^2 \quad (18)$$

For the ternary system, the self-consistency of the model is provided by calculating the bulk molar fractions of the solid and the liquid phases in equilibrium using the regular solution approximation. This calculation is performed by minimizing the free energy of the ternary system A–B–C at a temperature T and an overall composition of the biphase range (x_A, x_B, x_C) [13].

The free energy with reference to the pure liquid phase is minimized with respect to four independent variables and is written:

$$\Delta F = \sum_j \left(\sum_i (\lambda_{ii'}^j x_i^j x_{i'}^j)/2) + RT \sum_i (x_i^j \ln x_i^j) \right) + \sum_i x_i^S (\mu_i^{\circ S} - \mu_i^{\circ L})$$

with

$$\mu_i^{\circ S} - \mu_i^{\circ L} = \Delta\mu_i^\circ = -L_f^i \left(1 - \frac{T}{T_m^i}\right) \quad (19)$$

The equilibrium values of y_i^j are calculated by minimizing the free energy F of the solid–interface–liquid system. As the bulk molar fractions are fixed to their equilibrium values, the y_i^j values can be also calculated by minimizing the function σ (Equation 15).

4. Tensioactivity and adsorption

4.1. Reference state

The contribution due to the adsorption of the elements A, B and C at the interface will be given by the difference $\sigma^* - \sigma$ between the tension σ^* of a reference system in which the adsorption is zero and the interfacial tension σ (Equation 15). σ^* is found from Equation 15 by putting $y_i^j = x_i^j$:

$$\sigma^* \Omega_M = x_A^S \sigma_A^\circ \Omega_M + x_B^S \sigma_B^\circ \Omega_M + x_C^S \sigma_C^\circ \Omega_M + m \sum_{j \neq j'} (\lambda_{AB}^L x_A^j x_B^{j'} + \lambda_{BC}^L x_B^j x_C^{j'} + \lambda_{CA}^L x_C^j x_A^{j'}) - m \sum_j (\lambda_{AB}^j x_A^j x_B^j + \lambda_{BC}^j x_B^j x_C^j + \lambda_{CA}^j x_C^j x_A^j) \quad (20)$$

Note that σ^* corresponds to a purely dynamic interfacial tension of a solid–liquid system [9].

4.2. Tensioactivity

The tensioactivity of a component C at the interface of a solid A–liquid B binary system is characterized by its tendency to segregate at the interface from the liquid or solid phases, i.e. by the values of the ratio y_C^j/x_C^j. The equations giving y_C^j are obtained by minimizing the function $\sigma\Omega_M$ (Equation 15) with respect to four interfacial molar fractions y_B^S, y_C^S, y_A^L and y_C^L (B and C, and A and C being the minor elements, respectively, in the solid and in the liquid phase).

In order to obtain simple tensioactivity criteria, we calculate separately the adsorption in the liquid layer of the interface and that in the solid one with the simplifications $x_A^L \simeq 0$ and $x_B^S \simeq 0$.

In the liquid, for a small addition of C, the condition $\mathrm{d}\sigma/\mathrm{d}y_C^L = 0$ can be simply written by neglecting the adsorption in the solid layer ($y_i^S - x_i^S = 0$):

$$\ln \frac{y_C^L}{1-y_C^L} = \ln \frac{x_C^L}{1-x_C^L} + \frac{2l}{RT}(y_C^L - x_C^L)\lambda_{BC}^L - \frac{m}{RT}(\lambda_{CA}^L - \lambda_{AB}^L - \lambda_{BC}^L) \quad (21a)$$

In the same way, a second relationship gives the adsorption in the solid interfacial layer:

$$\ln \frac{y_C^S}{1-y_C^S} = \ln \frac{x_C^S}{1-x_C^S} + \frac{2l}{RT}(y_C^S - x_C^S)\lambda_{CA}^S - \frac{m}{RT}(\lambda_{BC}^L - \lambda_{AB}^L - \lambda_{CA}^S) + (\sigma_A^\circ - \sigma_C^\circ)\frac{\Omega_M}{RT} \quad (21b)$$

On dilution of the solute C in the two phases (i.e. $x_C^L \ll 1$ and $x_C^S \ll 1$), these equations are of the same type as the Fowler–Guggenheim [14] isotherms established for the adsorption on a solid

from the vapour:

$$x_C = \frac{y_C}{1-y_C} \exp\left(\frac{E_i y_C - E_a}{RT}\right) \qquad (22)$$

where E_a is the adsorption energy at infinite dilution and E_i the energy resulting from the interactions *into* the adsorption layer. For the adsorption from the liquid solvent (B) on to the solid layer ($x_C = x_C^L$ and $y_C = y_C^L$), we have:

$$E_a = m\tau_l = m(\lambda_{CA}^L - \lambda_{AB}^L - \lambda_{BC}^L)$$

$$E_i = 2l\lambda_{BC}^L$$

and for the adsorption from the bulk solid phase (A) in the solid layer, (i.e. $x_C = x_C^S$ and $y_C = y_C^S$):

$$E_a = m\tau_s = m\left[(\lambda_{BC}^L - \lambda_{AB}^L - \lambda_{CA}^S) + (\sigma_C^\circ - \sigma_A^\circ)\frac{\Omega_M}{m}\right]$$

$$E_i = 2l\lambda_{CA}^S$$

At infinite dilution, the tensioactivity of a solute C only depends on the τ_l and τ_s values. An average adsorption energy $m\bar{\tau}$ for the two kinds of adsorption sites can be defined:

$$\bar{\tau} = \frac{K_V\tau_l + \tau_s}{1 + K_V}$$

where K_V is the partition coefficient of C in the two phases, which can be written when A and B are mutually insoluble:

$$K_V = \frac{x_C^L}{x_C^S} = \exp\left(\frac{\lambda_{CA}^S - \lambda_{BC}^L + \Delta\mu_C^\circ}{RT}\right)$$

where $\Delta\mu_C^\circ$ is defined in Equation 19.

A necessary condition for the adsorption is $\bar{\tau} < 0$. As the terms τ_l and τ_s are generally of the same order of magnitude, if $K_V \gg 1$, $\bar{\tau} \simeq \tau_l$ and the adsorption is predominant in the liquid layer and vice versa.

In the case of $\bar{\tau} < 0$ (that is $y_C - x_C > 0$) at finite dilution of the solute C, the term E_i must be taken into account. According to the Equations 21 a and b, for positive values of λ_{BC}^L/RT and/or λ_{CA}^S/RT, the adsorption will be enhanced (see the curve a of Fig. 2), while for negative values of these parameters the adsorption will be weakened with increasing values of x_C (see curve c of Fig. 2).

The higher the negative value of $\bar{\tau}$, the higher the tensioactivity of C at infinite dilution. For positive values of $\bar{\tau}$, the solute C will desorb from the interface and the model predicts a nearly zero but slightly positive value of $(d\sigma/dx_C)_{x_C \to 0}$.

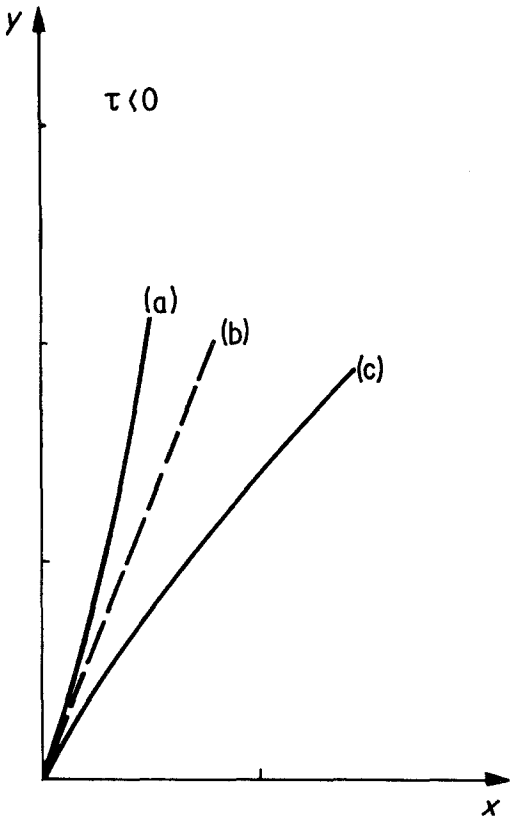

Figure 2 Schematic variation of the molar fraction of a ternary element in a liquid (or solid) interfacial layer versus the molar fraction of this element in the liquid or solid) bulk phase for $\tau_i < 0$ (or $\tau_s < 0$): (a) $\lambda_{BC}^L < 0$ (or $\lambda_{CA}^S > 0$); (b) $\lambda_{BC}^L = 0$ (or $\lambda_{CA}^S = 0$); (c) $\lambda_{BC}^L < 0$ (or $\lambda_{CA}^S < 0$).

5. Comparison between experimental results and calculations

5.1. Detailed results for the Fe–Pb–Cu system

We have chosen to detail the computed results for this system because the solid–liquid interfacial tension σ in Fe–Pb–Cu was measured at 1373 K in the whole range of concentration of the added element (copper) in the liquid phase [15]. At this temperature, the maximum solubility of lead in the solid iron is very small ($x_{(Pb)Fe}^S = 3 \times 10^{-6}$ [16]) as that of iron in the liquid lead ($x_{(Fe)Pb}^L = 8 \times 10^{-4}$ [17]), while iron and copper have little mutual solubility ($x_{(Cu)Fe}^S = 0.075$ and $x_{(Fe)Cu}^L = 0.033$ [18]).

For calculating σ we use the data reported in

TABLE I

(a) Thermodynamic data $\lambda_{ii'}$, of binary systems composing the ternary Fe–Pb–Cu and Fe–Ag–Cu; $\lambda^{S}_{ii'}$ are calculated from $\lambda^{L}_{ii'}$ and Equation 18

System ii'	$\lambda_{ii'}$ (kJ mol^{-1})	
	Solid	Liquid
Fe–Pb	151	104 [16, 17]
Pb–Cu	92	31.8-0.0081T [12]
Fe–Cu	40.9-0.0048T	43.25-0.0046T [12]
Fe–Ag	127-0.000 92T	105 [19]
Ag–Cu	31.4-0.0056T	19.7-0.0037T [12]

(b) Physico-chemical data for the pure components of the two systems in (a)

Element	σ° (mJ m^{-2})	T_m (K)	L_f (kJ mol^{-1})
Fe	254	1809	15.188
Pb	43	600.4	4.770
Cu	220	1356	13.054
Ag	143	1234	11.945

Table I: as all the binary thermodynamic data $\lambda^{j}_{ii'}$ (Table Ia), are not listed in the literature, they have been estimated; λ^{L}_{FePb} is calculated from the solubility of iron in liquid lead measured in the temperatures range between the eutectic and monotectic temperatures. λ^{S}_{FePb}, λ^{S}_{CuPb} and λ^{S}_{FeCu} are computed using Equation 18 from the corresponding values of $\lambda^{L}_{ii'}$, and the maximum solubility of the component i' in the solid i.

Note that even if there is a large error in the values of λ^{S}_{FePb} and λ^{S}_{PbCu}, the calculated phase diagram and σ will be almost unmodified because of the very weak solubility of lead in the iron and Fe–Cu solid solutions.

As the solid phase of the Fe–Pb–Cu system is nearly an Fe–Cu alloy, the value of the interfacial molar area Ω_M is

$$\Omega_M = \Omega^{Fe}_M \simeq \Omega^{Cu}_M = 3.6 \times 10^8 \text{ cm}^2 \text{ mol}^{-1}$$

In Fig. 3, the calculated and experimental interfacial tensions, σ, at 1373 K are plotted against the molar fraction of copper in the liquid phase (x^{L}_{Cu}): the values of σ given by the model agree rather well with the experimental results, equally as well in the field of small additions of copper where σ rapidly decreases, as in the more concentrated copper field where the diminishing of σ is very slow.

In Fig. 4, the five calculated quantities: σ, σ^*, $\sigma^* - \sigma$, y^{S}_{Cu} and y^{L}_{Cu} are plotted against x^{L}_{Cu}. The curve $\sigma^*(x^{L}_{Cu})$ shows the influence on σ of the

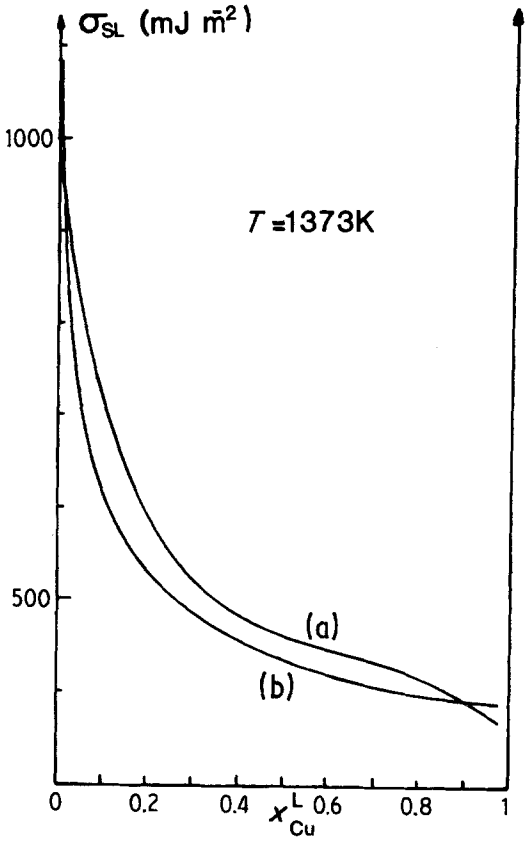

Figure 3 Calculated (a) and experimental (b) interfacial tension, σ, as a function of x^{L}_{Cu} at 1373 K for the ternary Fe–Pb–Cu.

only variation of the bulk phases compositions. The effect of the segregation is given by the difference $\sigma^* - \sigma$ (curve b) which takes a maximum value for $x^{L}_{Cu} \simeq 0.30$. These variations are explained by the two graphs (c) and (d) showing the interfacial molar fraction of the different components in the solid and liquid layers, respectively. As y^{S}_{Pb} and y^{L}_{Fe} are always very small ($y^{S}_{Pb} < 10^{-4}$ and $y^{L}_{Fe} < 0.03$) the solid layer composition can be described by means of only y^{S}_{Cu} and y^{S}_{Fe}, and that of the liquid layer by means of y^{L}_{Cu} and y^{L}_{Pb}. The curves show that when copper is added to the Fe–Pb system, this element rapidly segregates into both the solid and the liquid interfacial layers to the detriment of iron and lead, respectively. This can be explained by the fact that both τ_l and τ_s values are negative (see Table II). However, despite $|\tau_l| \simeq 7.7 > |\tau_s/K_V| \simeq 3.2$, the adsorption is weaker in the liquid layer than in the solid one. In fact these values of τ_l and τ_s/K explain the shape of the curves $y_{Cu} = f(x^{L}_{Cu})$ near $x^{L}_{Cu} = 0$, where $(y^{S}_{Cu}/x^{L}_{Cu})_{x_{Cu} \to 0}$ is less than $(y^{L}_{Cu}/x^{L}_{Cu})_{x_{Cu} \to 0}$.

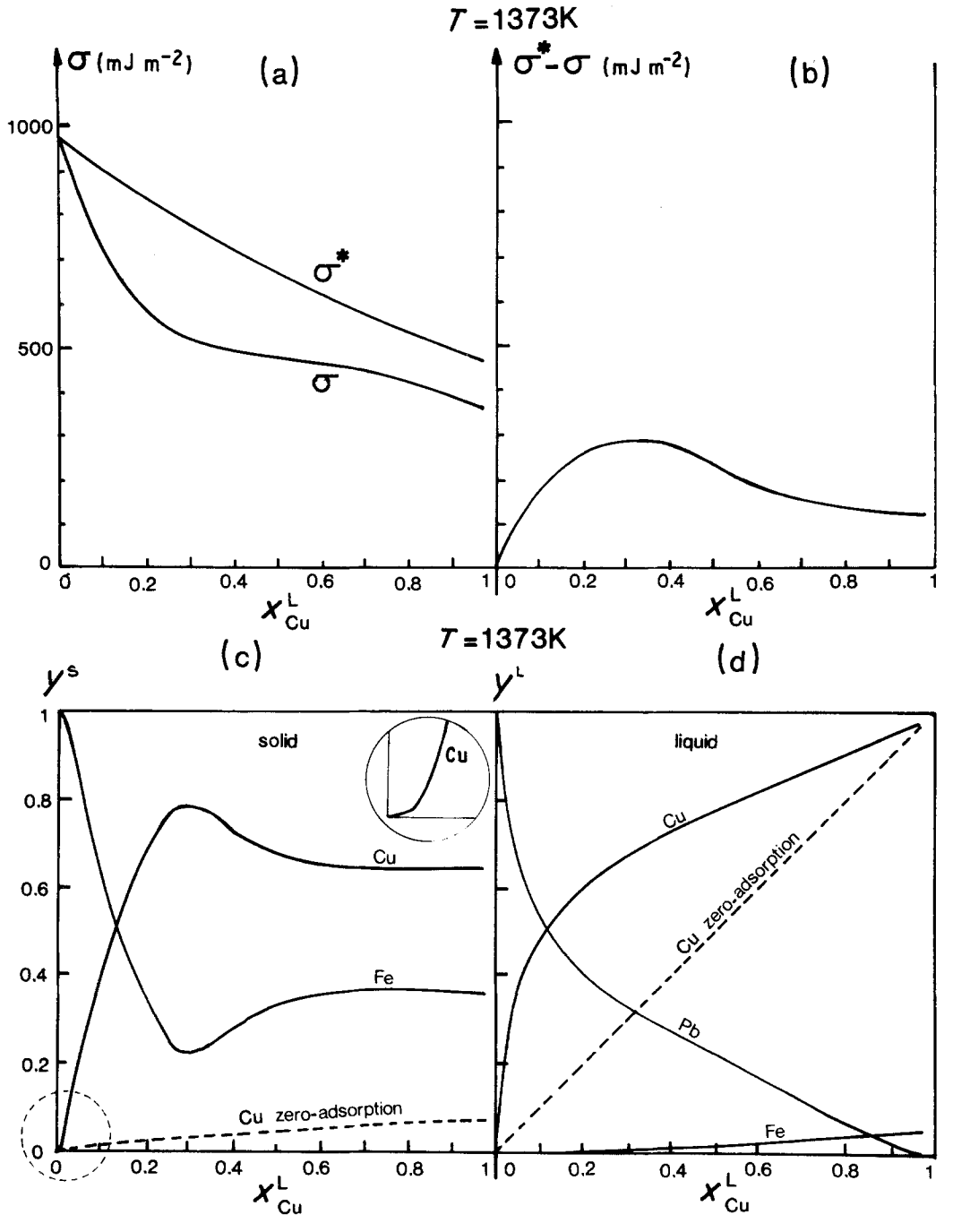

Figure 4 Calculated curves for the Fe–Pb–Cu system at 1373 K plotted against the molar fraction of copper in the liquid phase: (a) interfacial tensions σ and σ^* (at zero adsorption); (b) effect of the adsorption on the interfacial tension; (c) molar fractions of the components in the solid monolayer ($y^S_{Pb} = 0$); (d) molar fractions of the components in the liquid monolayer.

Moreover, this behaviour confirms the importance of the energetic term of interactions in the interfacial layer (E_i) which is more favourable for the adsorption in the solid layer than in the liquid one ($\lambda^S_{CA}/\lambda^L_{BC} \simeq 1.7$). The amplification of the term E_i as the temperature decreases, explains that the effect of the temperature on the adsorption of copper in the solid layer is more important than in the liquid layer as we can see from Fig. 5. These results show that a monolayer interfacial model

TABLE II All the thermodynamic data in liquid phase proceed from the Hultgren *et al.* compilation [12] except those of the binary systems marked with † (data of Miedema [19]). The $\lambda^{S}_{ii'}$ values are calculated from $\lambda^{L}_{ii'}$ and Equation 18. All these systems have a partition coefficient $K_V \gg 100$ except the systems marked as follows: (*, $K_V = 28.5$; ‡, $K_V = 3.36$; §, $K_V = 5.70$)

A–B–C system	T (K)	$\frac{\lambda^{L}_{AB}}{RT}$	$\frac{\lambda^{L}_{CA}}{RT}$	$\frac{\lambda^{L}_{BC}}{RT}$	$\frac{\lambda^{S}_{CA}}{RT}$	$\frac{\bar{\tau}}{RT}$	exp $(d\sigma/dx^{L}_{C})_{x_C \to 0}$ (mJ m^{-2})
Al–Pb–Sn	873	5.01	1.87	1.49		−4.63	− 1 300 [21]
Al–Bi–Sn	823	3.20	2.03	0.20		−1.37	− 200 [22]
Al–In–Sn	823	3.18	2.03	−0.36		−0.79	− 100 [23]
Al–Cd–Sn	823	4.10	5.29	1.31		≃ 0	0 [22]
Zn–Pb–Sn	605	4.28	1.70	1.86		−4.45	− 2 300 [24]
Zn–Bi–Cd*	631	3.31	1.66	0.27	3.55	> −2.11	− 16 [25]
Zn–Bi–In	609	3.45	2.27	1.28		> + 0.10	0 [26]
Fe–Pb–Cu‡	1373	9.11†	3.23	1.81	3.00	−8.39	−11 000 [15]
Fe–Ag–Cu§	1373	9.19†	3.23	1.28	3.00	−7.85	− 3 500 [20]
Fe–Pb–Ag	1373	9.11†	9.19†	0.48		≃ 0	0 [27]

would be insufficient to describe the adsorption of copper at the interface of the Fe–Pb–Cu system.

Figs. 6 and 7 show the results for the Fe–Ag–Cu system, the phase diagram of which is quite similar to that of Fe–Pb–Cu system. The σ measurements were made by Pique *et al.* [20]; the data used to compute the interfacial quantities are reported in the Table I (as experimental thermodynamic data do not exist for the Fe–Ag system, we use the calculated enthalpy of mixing given by Miedema *et al.* [19]). The detailed results are not presented because they are quite similar to those obtained for the Fe–Pb–Cu system. Indeed, as for this system, Fig. 6 shows that σ decreases rapidly for the first additions of copper in the liquid phase, then slowly for higher values of x^{L}_{Cu}.

The model correctly reproduces the variations of σ with x^{L}_{Cu} in spite of an underestimation of the amplitude of σ. Moreover, in Fig. 7, the "experimental" number, N^{exp}_{Cu}, of equivalent monolayers of copper at the interface and the calculated number of the same ($N^{cal}_{Cu} = y^{S}_{Cu} + y^{L}_{Cu}$) as a function of the ratio $K = x^{L}_{Cu}/(x^{L}_{Cu} + x^{L}_{Ag})$ are compared. N^{exp}_{Cu} is evaluated from the experimental curve $\sigma(x^{L}_{Cu})$ using the Gibbs isothermal adsorption equation [20]: we can consider that the agreement between the two curves is fairly good, taking into account the experimental error on N^{exp}_{Cu} and the numerous approximations of the model.

5.2. Tensioactivity criteria for some systems with aluminium, zinc, iron-based solid phases

The factor $\bar{\tau}$ previously defined (Section 4.2) enables us to know in advance if a ternary element C is tensioactive or not at the interface of an A solid–B liquid system.

We have computed $\bar{\tau}$ for some ternary systems, the solid–liquid interfacial tension of which was measured as a function of the molar fraction of the ternary element C. For each of these systems, Table II gives the experimental value of the slope $(d\sigma/dx^{L}_{C})_{x_C \to 0}$ (known with an uncertainty of 30%), the value of $\bar{\tau}$ and the thermodynamic data used to compute it.

In all the systems presented, the solubility of B in the solid phase A is negligible. On the liquid side, in all the systems the solubility of A in the liquid phase B is small ($x^{L}_{(A)B} < 0.05$) except for the two systems Zn–Bi–X (X = Cd or In) in which $x^{L}_{(Zn)Bi} \simeq 0.20$. For these two systems, the tensioactivity (determined by the value of $\bar{\tau}$ calculated for an A–B–C system in which A and B are mutually insoluble) is clearly overestimated. For all these systems, except the Zn–Bi–Cd, Fe–Pb–Cu and Fe–Ag–Cu ones, C is quite insoluble in the A solid, the partition coefficient K being very large ($K_V \gg 10^2$) such that $\bar{\tau}$ is nearly equal to τ_1 (i.e. adsorption is possible only in the liquid layer of the interface).

5.3. Discussion

In Fig. 3a we saw that the theoretical curve $\sigma = f(x^{L}_{Cu})$ for the Fe–Pb–Cu system showed three distinct ranges of variation of the slope $d\sigma/dx^{L}_{Cu}$: for the first additions of copper, a sharp decrease of σ was followed by a smooth diminishing and again a larger decrease near the limit solubility of copper in the liquid phase; but, on the experimental

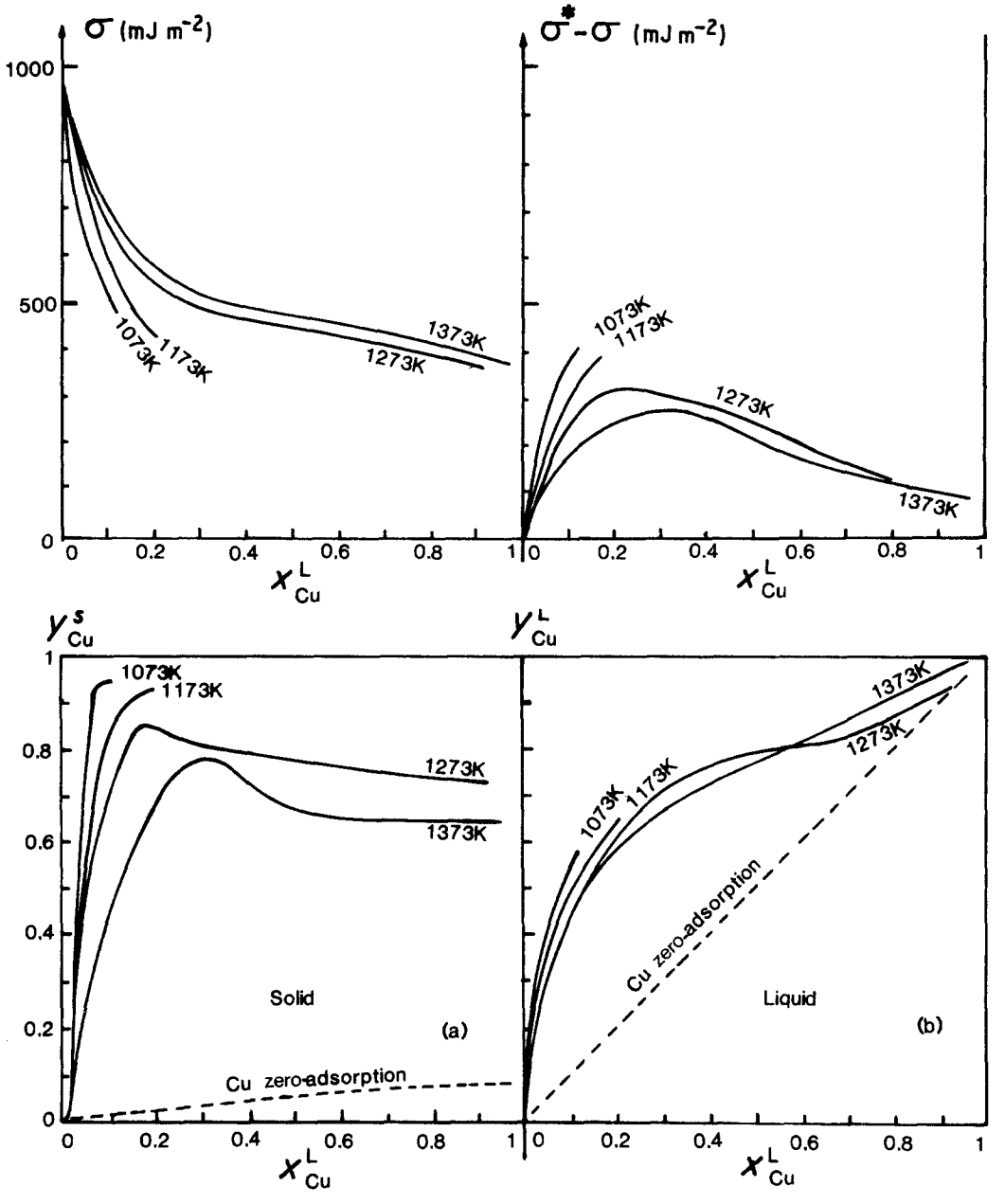

Figure 5 Effect of the temperature on the calculated interfacial tension and molar fractions in the interfacial layers as a function of x^{L}_{Cu} for the Fe–Pb–Cu system.

curve, only the two first ranges appear. The uncertainty on the σ measurements which is as large as the variation of σ itself in the copper concentrated range, is responsible for the lack of the third range in the Fe–Pb–Cu system. Effectively, in many other systems such as Fe–Ag–Cu (Fig. 6), Zn–Pb–Sn [24], Al–Bi–Sn [22], Al–Pb–Sn [21], the three $d\sigma/dx_C$ ranges are also found by calculation as well as experimentally. As an example, we indicate the Zn–Pb–Sn system; In Fig. 8, the interfacial tension between solid zinc and liquid Pb–Sn, and the molar fraction x^{L}_{Zn} are plotted against the molar fraction of added element in the liquid phase (x^{L}_{Sn}). The first range P corresponds to the adsorption of tin at the interface Zn–Pb. In the second range Q, the interface is saturated in tin and σ is nearly constant. Finally, in the third range R, σ again rapidly decreases because of an important variation in the concentration of the liquid bulk phase as shown on the curve $x^{L}_{Zn} = f(x^{L}_{Sn})$.

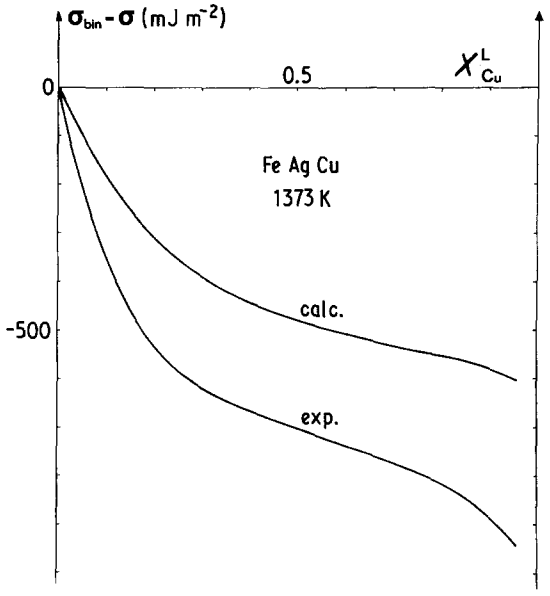

Figure 6 Calculated and experimental values of ($\sigma_{bin} - \sigma$) at 1373 K as a function of the molar fractions of copper in the liquid phase (σ_{bin} = interfacial tension of the binary Fe–Ag system; σ = interfacial tension of the ternary Fe–Ag–Cu system).

The first range (adsorption range) only exists if $\bar{\tau}$ is clearly negative, otherwise, as for the Zn–Bi–Cd system [25], only the two last ranges of σ variation (Q and R) are present.

The results in Table II show that only the systems having high negative values of $\bar{\tau}/RT$ (i.e. Al–Pb–Sn, Zn–Pb–Sn, Fe–Pb–Cu and Fe–Ag–Cu) exhibit a rather large decrease in σ as soon as the first amounts of C are added to the A–B system. In the other cases, the adsorption effects are either small or negligible. Moreover, in agreement with the experimental results, the tensioactivity predicted by the model decreases in the following orders:

$$\text{Al–Pb–Sn} \gg \text{Al–Bi–Sn} > \text{Al–In–Sn}$$

$$> \text{Al–Cd–Pb} \simeq 0$$

$$\text{Zn–Pb–Sn} \gg \text{Zn–Bi–Cd} \simeq \text{Zn–Bi–In} \simeq 0$$

$$\text{Fe–Pb–Cu} > \text{Fe–Ag–Cu} \gg \text{Fe–Pb–Ag} \simeq 0$$

All the examples presented show that at solid–liquid interfaces of binary systems, the tensioactivity of an infinitely dilute third element is never as large as that at solid–solid and solid–vapour interfaces (see Table III). At solid–liquid interfaces, the tensioactivity mainly results from chemical interactions (as for liquid–liquid interfaces) while for grain boundaries and free surfaces, the cohesion and lattice strain energies are the two factors mainly responsible for the segregation [28]. For this reason, in contrast to solid–vapour, liquid–vapour or grain-boundary interfaces for which an important reduction of the corresponding interfacial tension can be obtained with tensioactive solutes in the concentration range of 0.1% or less, tensioactive effects of the same magnitude of a solute C at a solid A–liquid B interface require additions of 1% or more. In this range of concentration, the energetic interactions *in* the adsorption layers (E_i) are no more negligible and in order to be highly tensioactive, a solute C must be such that $\tau \ll 0$ and λ^S_{CA} and/or $\lambda^L_{BC} \gg 0$.

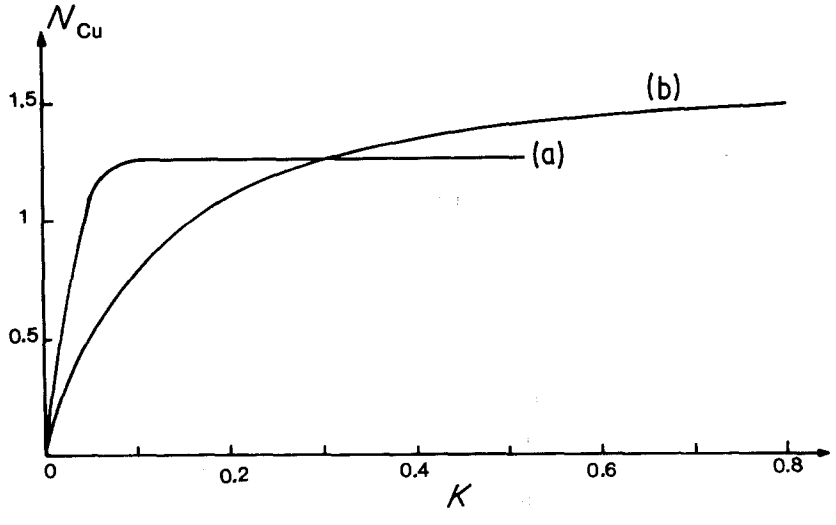

Figure 7 Experimental (a) and calculated (b) numbers of equivalent monolayers of copper at the solid–liquid interface of the Fe–Ag–Cu system at 1373 K, as a function of the ratio $K = x^L_{Cu}/(x^L_{Cu} + x^L_{Ag})$.

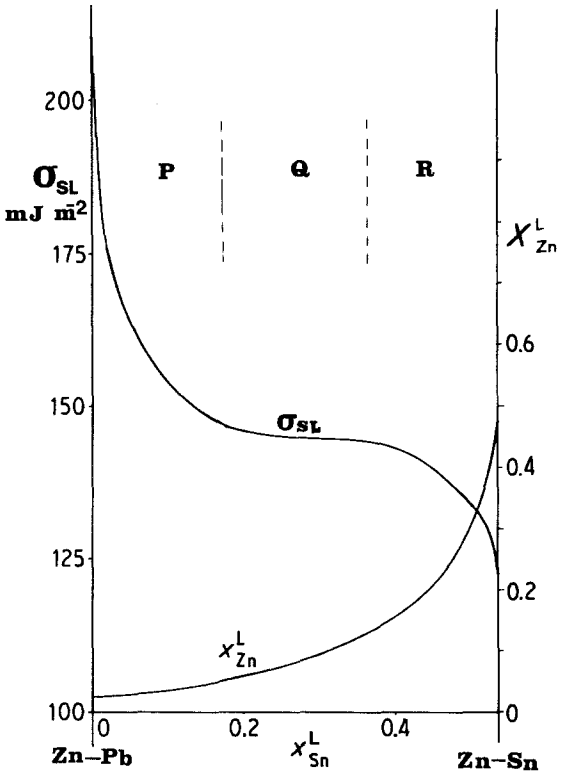

Figure 8 Experimental interfacial tension isotherm of the solid zinc–liquid (Pb–Sn) system [25].

As we have noted above, the present model is, in principle, applicable only in the low temperature range of the solid–liquid phase diagram, i.e. at temperatures much lower than the melting temperature, T_m, of the major element A of the solid solution ($T < 0.75\,T^A_m$). Indeed, at temperatures close to T_m, the solid–liquid interfaces are no more atomically smooth and the roughness of the interface must be taken into account in the segregation calculation. This is possible, for example, by combining the present model with the two layers model of Mutaftschiev [31] for atomic roughness of pure components. However, the complexity of such a calculation is not justified, given that the atomic roughness has rather little influence on the segretagion [10] (although the segregation has considerable influence on the roughness). In other words, the segregation criteria established in this paper can be used in a qualitative way even in the high temperature range of the phase diagram.

Moreover, in the model, we have neglected the local chemical ordering effects on the interfacial tension and segregation. These effects can be taken into account by using for example, Guggenheim's first order statistics. However, the influence of local chemical ordering on the interfacial tension and adsorption is generally weak in comparison with the experimental uncertainty of these qualities, as shown elsewhere [30].

6. Conclusion

The two-layer interface model allows the calculation of the interfacial tension and adsorption of solid A–liquid B–solute C system, given the exchange energies of the three binary liquid alloys (AB, BC and AC), and the corresponding phase diagrams. This model correctly predicts the three possible ranges of the σ versus x^L_C curve at constant temperature. Taking $\sigma(A–B) > \sigma(A–C)$, an adsorption range (P, Fig. 8) is found where σ rapidly decreases with the first additions of C in the A–B system, along with an intermediate range (Q, Fig. 8) corresponding to a saturation of the interface, where σ decreases very slowly with the concentration, and a terminal range (R, Fig. 8), where σ decreases again rapidly, that is mainly due to the changes in the bulk phase compositions.

The first adsoprtion range exists only if the value of $\bar{\tau}$ (the average energy of adsorption of the solute C at *infinite dilution*) is negative: the more $\bar{\tau}$ is negative, the more the decrease of σ with the first additions of C is clearly defined.

TABLE III Slope $(d\sigma/dx_C)_{x_C \to 0}$ for different kinds of interfaces

system A–B	Interface (S = solid L = liquid)	T (K)	Solute C	$\left(\frac{d\sigma}{dx_C}\right)_{x_C \to 0}$ (mJ m^{-2})	Reference
Fe–Fe	S–S	1693	Sn	-10^5	[28]
Cu–Cu	S–S	1223	Sb	-10^5	[29]
Fe–Ag	S–L	1373	Cu	-3.5×10^3	[20]
Fe–Pb	S–L	1373	Cu	-1.1×10^4	[15]
Zn–Pb	S–L	605	Sn	-2.2×10^3	[24]
Zn–Pb	L–L	701	Sn	-1.2×10^3	[24]
Zn–Pb	L–L	701	In	-6×10^2	[30]

The study of the interfacial activity of ternary elements in some systems with iron, aluminium or zinc-based solid phases shows that the values of $\bar{\tau}$ are in good agreement with the experimental tensio-activity order in each series.

The adsorption energy for the solid–liquid interfaces is mainly due to the chemical interaction effects which are very much weaker than those which exist for solid–vapour interfaces or grain boundaries (in which cohesion and elastic strain energies predominate). As a consequence, a strong decrease of the solid–liquid interfacial tension cannot be obtained with additions of C as small as for the other kinds of interfaces, but requires additions of 1% or more.

References

1. N. EUSTATHOPOULOS, J. C. JOUD and P. DESRE, *J. Chim. Phys.* **69** (1972) 1599.
2. *Idem, ibid.* **71** (1974) 777.
3. D. NASON and W. A. TILLER, *Surf. Sci.* **40** (1973) 109.
4. A. R. MIEDEMA and F. J. A. DEN BROEDER, *Z. Metallkde* **70** (1979) 14.
5. R. WARREN, *J. Mater. Sci.* **15** (1980) 2489.
6. D. CAMEL, J. P. SIMON and N. EUSTATHOPOULOS, *Scripta Metall.* **14** (1980) 1101.
7. A. PASSERONE and N. EUSTATHOPOULOS, *Acta Metall.* **30** (1982) 349.
8. L. COUDURIER, N. EUSTATHOPOULOS and P. DESRE, *Fluid Phase Equilibria* **4** (1980) 71.
9. R. DEFAY, I. PRIGOGINE, A. BELLEMANS and D. H. EVERETT, "Surface tension and adsorption" (Longmans, London, 1966).
10. L. COUDURIER, A. PASSERONE and N. EUSTATHOPOULOS, *Acta Metall.* **26** (1978) 465.
11. N. EUSTATHOPOULOS, *Int. Met. Rev.* **28** (1983) 189.
12. R. HULTGREN, P. D. DESAI, D. T. HAWKINS, M. GLEISER and K. K. KELLEY, "Selected values of the thermodynamic properties of binary alloys" (American Society for Metals, Ohio, 1973).
13. I. ANSARA, *Int. Met. Rev.* **1** (1979) 20.
14. R. H. FOWLER and E. A. GUGGENHEIM, "Statistical thermodynamics" (Cambridge University Press, 1939) p. 429.
15. O. GOMEZ-MORENO, L. COUDURIER, N. EUSTATHOPOULOS and P. DESRE, *Comp. Rend. Acad. Sci.* **289** (1979) 141.
16. F. A. SHUNK, "Constitution of Binary Alloys" (McGraw Hill, New York, 1969).
17. D. A. STEVENSON and J. WULFF, *Trans. Met. Soc. AIME* **221** (1961) 271.
18. M. HANSEN and H. ANDERKO, "Constitution of Binary Alloys" (McGraw Hill, New York, 1958).
19. A. R. MIEDEMA, F. R. DE BOER and R. BOOM, *Calphad* **1** (1977) 341.
20. D. PIQUE, L. COUDURIER and N. EUSTATHOPOULOS, *Scripta Metall.* **15** (1981) 165.
21. O. RELAVE, Diplôme d'Etudes Approfondies, Grenoble (1983).
22. K. K. IKEUYE and C. S. SMITH, *Trans. AIME* **185** (1949) 762.
23. N. EUSTATHOPOULOS, L. COUDURIER, J. C. JOUD and P. DESRE, *J. Chim. Phys.* **71** (1974) 1465.
24. D. CHATAIN, C. VAHLAS and N. EUSTATHOPOULOS, *Acta Metall.* **32** (1984) 227.
25. C. VAHLAS and N. EUSTATHOPOULOS, *J. Chim. Phys.* **80** (1983) 515.
26. A. PASSERONE, R. SANGIORGI and N. EUSTATHOPOULOS, *Scripta Metall.* **14** (1980) 1089.
27. O. GOMEZ-MORENO, thesis, University of Grenoble, (1978).
28. M. P. SEAH and E. D. HONDROS, *Proc. R. Soc.* **A335** (1973) 191.
29. M. C. INMAN, D. Mc. LEAN and H. R. TIPLER, *ibid.* **A273** (1963) 538.
30. D. CHATAIN and N. EUSTATHOPOULOS, *J. Chim. Phys.* **81** (1984) 599.
31. B. MUTAFTSCHIEV, "Adsorption et Croissance Cristalline", Colloque International CNRS No. 152, CNRS, Paris (1965).

Received 23 July
and accepted 6 September 1984